Scripta Materialia 211 (2022) 114516

Contents lists available at ScienceDirect

Scripta Materialia

journal homepage: www.elsevier.com/locate/scriptamat

Ultra-low temperature spark plasma sintering of super wear-resistant hard B_4C composites

Victor Zamora, Fernando Guiberteau, Oscar Borrero-López, Angel L. Ortiz*

Departamento de Ingeniería Mecánica, Energética y de los Materiales, Universidad de Extremadura, Badajoz 06006, Spain

ARTICLE INFO

Article history:
Received 14 December 2021
Revised 7 January 2022
Accepted 10 January 2022
Available online 17 January 2022

Keywords:
B_4C
Hard ceramic composites
Super-low-wear ceramic composites
Spark plasma sintering
Liquid-phase sintering

ABSTRACT

The feasibility was investigated of fabricating super wear-resistant hard B_4C composites by spark plasma sintering (SPS) at ultra-low temperature (*i.e.*, 1400 °C) using very high proportions of $MoSi_2$ aids (*i.e.*, 35–50 vol.%). It is shown that with 40 vol.% $MoSi_2$ aids already sufficient Si transient liquid phase is formed *in situ* during SPS (by the reaction $B_4C+2MoSi_2 \rightarrow SiC+2MoB_2+3Si$) to achieve the ultrafast full densification of B_4C at 1400 °C, the Si melting point, simply by pore filling, particle rearrangement, and liquid spreading. Importantly, it is also shown that the resulting B_4C composites are hard (*i.e.*, ≈23 GPa) and super wear-resistant (*i.e.*, ~10^7 (N·m)/mm^3), attributes both deriving from the composites' quadruplex-particulate (*i.e.*, B_4C plus β-SiC, β-MoB_2, and $MoSi_2$), fine-grained (*i.e.*, <1 μm), fully-dense microstructure. Thus, this work opens a new avenue for the present and future lower-cost fabrication of novel B_4C composites for use in contact-mechanical and tribological applications.

Hard ceramics, understood as those with hardnesses above 20 GPa, are needed in myriad engineering applications requiring high contact-damage and wear resistances (*e.g.*, bearings, valves, nozzles, gears, mechanical seals, armour panels, *etc.*) [1,2]. They are mostly carbides, nitrides, and borides, some developed in the past few decades (*e.g.*, SiC, Si_3N_4, ZrB_2, *etc.*) and others more recently (*e.g.*, B_4C, ZrC, *etc.*) [1,2]. Besides being hard or superhard, these ceramics are also ultra-refractory and therefore virtually undensifiable by solid-state sintering. Consequently, they are usually densified by liquid-phase sintering (with or without pressure), but requiring more demanding sintering conditions than used for the solid-state sintering of the typical oxide structural ceramics (*e.g.*, ZrO_2, Al_2O_3, TiO_2, *etc.*).

B_4C is an outstanding hard ceramic. Known as "black diamond", it is the third hardest compound discovered so far, and can be synthesized routinely in the tons required for the mass fabrication of ceramic pieces [3,4]. It is so extremely hard that it is classed as ultrahard, a subfamily of the hard materials with hardnesses above 30 GPa. Recently, it has been demonstrated that B_4C can be densified at smoother conditions by spark plasma sintering (SPS) with metal disilicides ($MeSi_2$'s) [5–7]. This is because $MeSi_2$'s act as reactive sintering additives forming *in-situ* Si (*i.e.*, $B_4C+2MeSi_2 \rightarrow SiC+2MeB_2+3Si$), which is a transient phase that first melts promoting densification by liquid-phase sintering and then disappears forming more SiC (*i.e.*, $Si+C \rightarrow SiC$) [5,6]. Triple-particulate, ultrahard (>30 GPa), toughened (>~4 MPa·$m^{0.5}$) B_4C-SiC-MeB_2 composites have thus been SPS-ed at temperatures unattainably low for densifying pure B_4C [5–7] (*i.e.*, at 1700 °C). Transient-liquid phase assisted SPS of B_4C has also been achieved with Ti-Al aids (with the resulting composites having high values of hardness (>30 GPa), toughness (>5 MPa·$m^{0.5}$), flexural strength (>500 MPa), and wear resistance (≥10^7 (N·m)/mm^3)) [8–14].

The three studies that there have been so far on SPS of B_4C with $MeSi_2$'s were aimed at maximizing the mechanical properties, especially the ultra-high hardness, of the resulting B_4C-SiC-MeB_2 composites by optimizing the proportion of $MeSi_2$ aids [5–7]. Thus, ultrahard B_4C-SiC-MoB_2 (~33 GPa) and B_4C-SiC-TiB_2 (~34 GPa) composites were fabricated by SPS-ing B_4C with 20 vol.% $MoSi_2$ at 1700 °C [7] and with 12 wt.% $TiSi_2$ at 1800 °C [6], respectively. Alternatively, because densification of these B_4C composites is assisted by the formation *in situ* of transient molten Si, it is worth exploring whether the proportion of $MeSi_2$ aids can also be optimized to yield dense B_4C-SiC-MeB_2 composites by SPS at only ~1400 °C, the Si melting point.[1] The aim would be to use greater proportions of $MeSi_2$ aids than before (*i.e.*, >30 vol.%) to form enough transient Si as to densify B_4C by SPS at 1400 °C only by pore filling, particle rearrangement, and liquid spreading. Although likely softer than the current ultrahard B_4C-SiC-MeB_2 composites, the feasibility of fabricating still very hard (*i.e.*, ≥20 GPa), super-low-wear (*i.e.*, ≲10^{-6} mm^3/(N·m)) B_4C composites at such a low

* Corresponding author.
E-mail address: alortiz@unex.es (A.L. Ortiz).

[1] The Si melting point is ~1410 °C, but in SPS the actual temperature of the powder compact is higher than measured by the optical pyrometers.

https://doi.org/10.1016/j.scriptamat.2022.114516

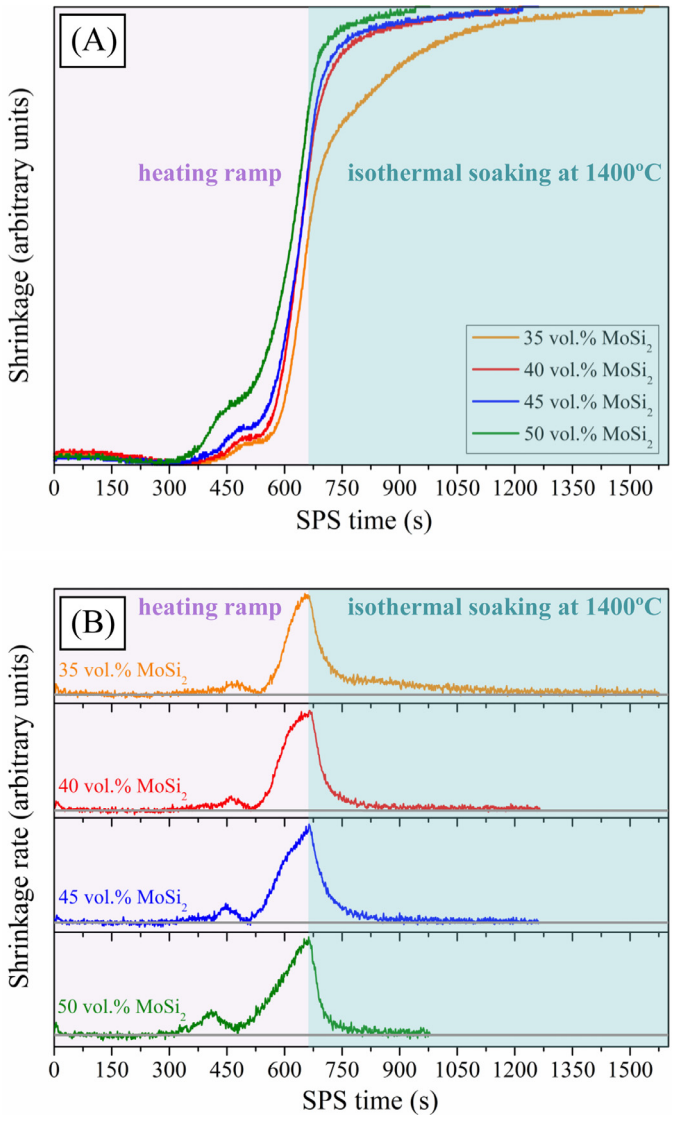

Fig. 1. Curves of (A) shrinkage and (B) shrinkage rate as functions of time, once corrected for the expansion of the graphite parts, logged during the SPS tests with target temperature of 1400 °C for the four B_4C+$MoSi_2$ powder batches, as indicated. The regimes of non-isothermal heating (*i.e.*, heating ramp up to 1400 °C at 100 °C/min) and of isothermal heating (*i.e.*, soaking at 1400 °C) are distinguished. Isothermal soaking time was 15, 10, 10, and 5 min for 35, 40, 45, and 50 vol.% $MoSi_2$ aids, respectively. The flat lines in (B) are baselines. The SPS time count started from the application of the 75 MPa pressure at 300 °C.

SPS temperature is tantalizingly appealing. Whether or not this is possible is investigated here for B_4C SPS-ed with $MoSi_2$ aids.

Powders of B_4C (Grade HD20, H.C. Starck; d_{50} ~0.3–0.6 μm) and $MoSi_2$ (Grade B, H.C. Starck; d_{50} ~3.5–5 μm) were mixed in relative proportions of 65+35, 60+40, 55+45, and 50+50 vol.%. The powder mixtures were then SPS-ed (HP-D-10, FCT Systeme GmbH) within graphite dies (2 cm diameter) in dynamic vacuum at 1400 °C (as measured by an axial optical pyrometer, and reached at 100 °C/min) and 75 MPa pressure (applied at 300 °C), for the time needed for the shrinkage curve to flatten. The resulting B_4C composites, hereafter termed "Comp-B_4C-x%$MoSi_2$" (with x = 35, 40, 45, or 50), were ground and diamond polished to a 0.25 μm finish.

Fig. 1 shows the shrinkage (Fig. 1A) and shrinkage-rate (Fig. 1B) curves as functions of the SPS time for the four B_4C+$MoSi_2$ powder batches. It is seen in Fig. 1A that there is a first shrinkage jump centred at ~460–510 s,[2] corresponding to SPS temperatures of ~1065–1150 °C, after which the shrinkage suddenly accelerates to then tend gradually, already during the soaking at 1400 °C, towards the maximum possible shrinkage. It is seen in Fig. 1B that the maximum shrinkage rate always occurs at ~662±4 s, corresponding to the first seconds of soaking at 1400 °C. Note that ~1065–1150 °C are the onset SPS temperatures for the reaction $B_4C+2MoSi_2 \rightarrow SiC+2MoB_2+3Si$ [5], and ~1400 °C corresponds to the Si melting point. Importantly, it is also seen in Fig. 1A that the sinterability increases, to a greater or lesser extent, with increasing proportion of $MoSi_2$ aids because (i) there is greater shrinkage (*i.e.*, densification) at the same SPS time (*i.e.*, temperature) and (ii) less soaking time at 1400 °C is required for the shrinkage curve to flatten (*i.e.*, the ultimate densification is reached sooner). This is due to the greater formation of Si with increasing $MoSi_2$ proportion. Indeed, according to the reaction $B_4C+2MoSi_2 \rightarrow SiC+2MoB_2+3Si$, the nominal abundances of Si formed during SPS when using 35, 40, 45, and 50 vol.% $MoSi_2$ aids are ~23.19, 26.32, 29.39, and 32.43 vol.%, respectively.

Also importantly, the shrinkage-rate curves in Fig. 1B confirm that densification occurred by liquid phase sintering (LPS) essentially, with only stages of pore filling, particle rearrangement, and liquid spreading, and little or negligible solution-reprecipitation. Indeed, according to LPS theory, upon melt formation there is a densification burst, with full densification being possible if enough liquid is formed [15,16]. The shape of the shrinkage-rate curves, flattening very quickly after the abrupt peak at 1400 °C attributable to molten Si, is proof of this. Indeed, the shape of these shrinkage-rate curves differs from that of those reported for Comp-B_4C-x%$MoSi_2$ fabricated with lower proportions of $MoSi_2$ aids ($x \leq 15$) because in the latter, given the insufficient molten Si formed (*i.e.*, only ~3.46, 6.88, and 10.24 vol.% Si for 5, 10, and 15 vol.% $MoSi_2$ aids), there is also an ultimate stage of densification by solid-state sintering [5].

Fig. 2A–D show moderate-magnification scanning electron microscopy (SEM; S-3600 N, Hitachi) images representative of the fracture surface of Comp-B_4C-x%$MoSi_2$ (x=35–50). It is seen that whereas Comp-B_4C-35%$MoSi_2$ (Fig. 2A) is slightly porous (*i.e.*, ~5%), Comp-B_4C-40%$MoSi_2$ (Fig. 2B), Comp-B_4C-45%$MoSi_2$ (Fig. 2C), and Comp-B_4C-50%$MoSi_2$ (Fig. 2D) are all three fully dense. Therefore, it is clear that at least ~40 vol.% $MoSi_2$ aids is needed to fully densify B_4C by SPS at 1400 °C (under 75 MPa).[3] This led to the nominal formation of ~26.32 vol.% molten Si if all the $MoSi_2$ was consumed, and less if not. Interestingly, Fig. 2A–D also show that Comp-B_4C-x%$MoSi_2$ (x=35–50) have complex fine-grained multiparticulate microstructures, with a lower and greater relative abundances of B_4C (darker-grey phase) and Si/Mo-rich second phases (whiter and lighter-grey phases), respectively, as the proportion of $MoSi_2$ aids increases (confirmed in Supplementary Figs. SI1 and SI2). The fine grain size[4] (*i.e.*, <1 μm) is because SPS at 1400 °C promoted densification with little, if any, coarsening by solution-reprecipitation.

According to the X-ray diffraction (XRD; D8 Advance, Bruker AXS) patterns shown in Fig. 2E, the Si/Mo-rich second phases are β-SiC, β-MoB_2, and $MoSi_2$. However, there is no Si, which proves that densification occurred by transient LPS [15,16]. SiC and MoB_2

[2] Specifically, at ~460 s (or 1065 °C), 490 s (or 1115 °C), 500 s (or 1135 °C), and 510 s (or 1150 °C) for 50, 45, 40, and 35 vol.% $MoSi_2$, respectively.

[3] Prolonging the SPS time of Comp-B_4C-35%$MoSi_2$ at 1400 °C beyond 15 min would not have resulted in further densification, which requires the use of a slightly higher SPS temperature.

[4] There are, however, some larger grains in the microstructures (Supplementary Fig. SI1), identified as MoB_2 grains by EDS (Supplementary Fig. SI2). Also, these grains are more abundant with increasing proportion of $MoSi_2$ aids (Supplementary Fig. SI1).

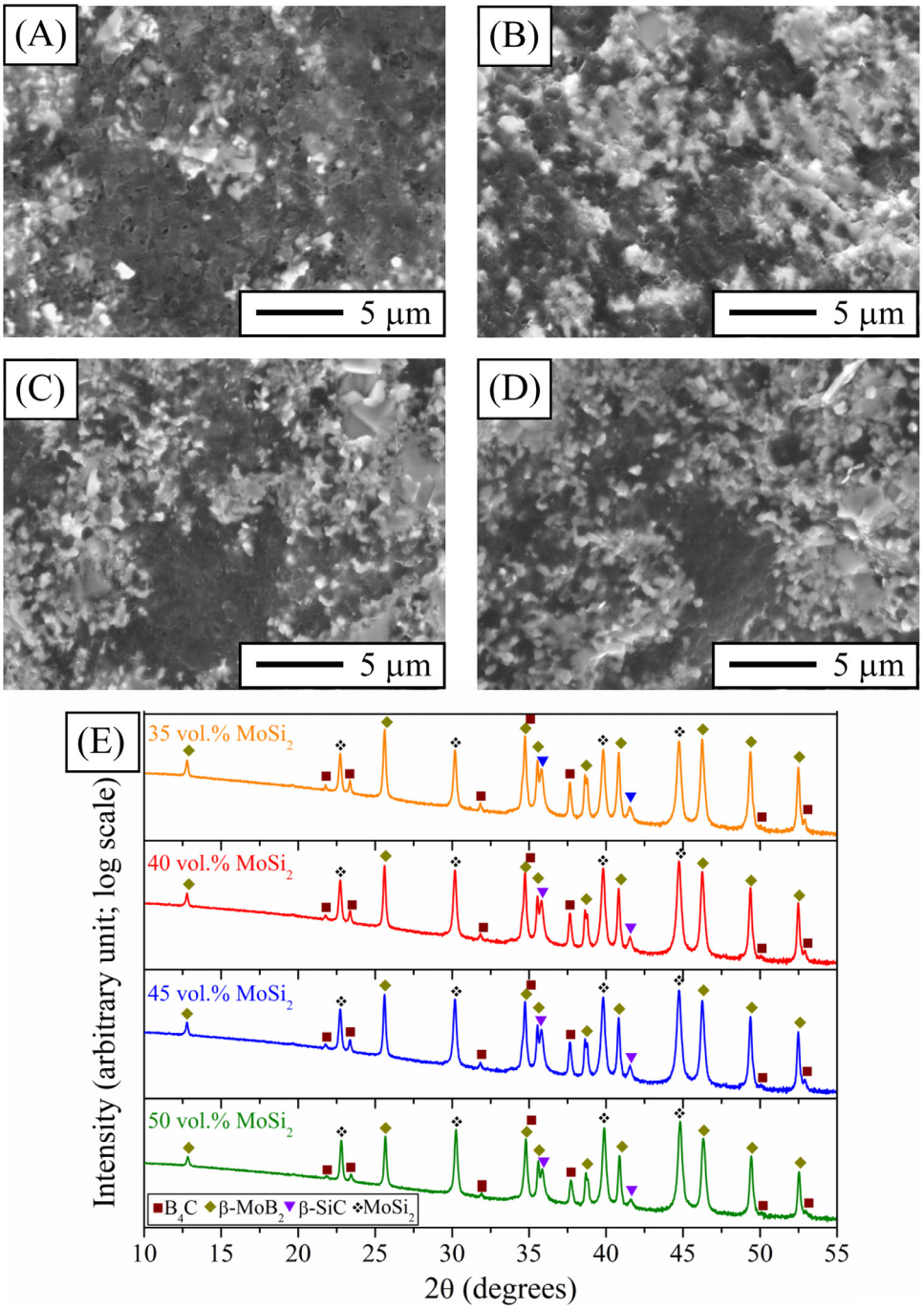

Fig. 2. Moderate-magnification SEM image representative of the fracture surface of (A) Comp-B_4C-35%$MoSi_2$, (B) Comp-B_4C-40%$MoSi_2$, (C) Comp-B_4C-45%$MoSi_2$, and (D) Comp-B_4C-50%$MoSi_2$. Imaging was done with secondary electrons at 15 kV. (E) XRD patterns of Comp-B_4C-x%$MoSi_2$ (x=35–50), as indicated. Peak assignations are included. The XRD patterns were acquired with pure Cu$K\alpha_1$ incident radiation and were indexed using the PDF2 database. The intensity scale is logarithmic to facilitate observation of the weaker peaks.

are the reaction products expected when B_4C reacts with $MoSi_2$ and all the transient Si is consumed to form more SiC, whereas the unreacted $MoSi_2$, which in this case is the limiting reactant, is due to the slow reaction kinetics at 1400 °C. One implication is then that the abundances of molten Si formed *in situ* during SPS are lower than the nominal ones, but, albeit less than 26.32 vol.%, still sufficient in Comp-B_4C-40%$MoSi_2$ to achieve full densification by pore filling, particle rearrangement, and liquid spreading. This is because the solid particles are not monosized spheres and therefore pack above 74%, so less than 26 vol.% liquid phase is actually required. Another implication is that Comp-B_4C-x%$MoSi_2$ (x=35–50) are quadruplex-particulate composites, not triplex-particulate composites as were those fabricated in earlier work with up to 25 vol.% $MoSi_2$ aids [7].

Consumption of all the $MoSi_2$ seems unlikely if the aim is to fabricate these B_4C composites at only 1400 °C. First, less than 40 vol.% $MoSi_2$ aids cannot be used because then full densification is not achieved at 1400 °C. Second, prolonging the SPS time (*i.e.*, the soaking time at 1400 °C) is impractical because it has no effect on the reaction kinetics. Third, using higher SPS temperatures deviates from the processing goal pursued, and is not a solution because even Comp-B_4C-30%$MoSi_2$ SPS-ed at 1700 °C con-

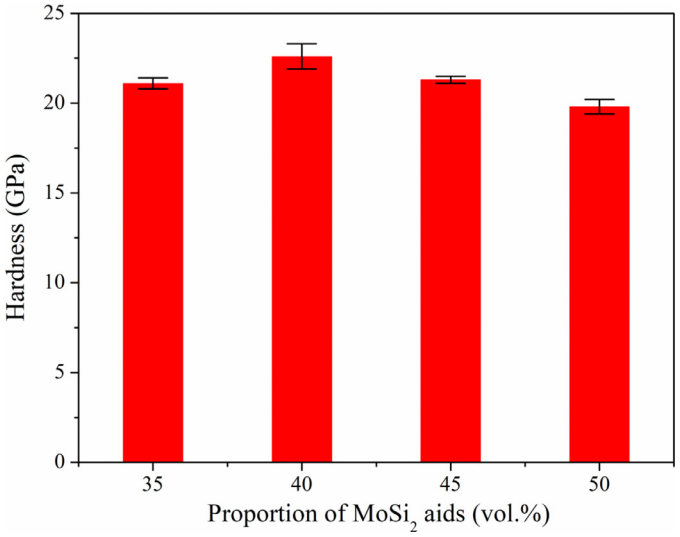

Fig. 3. Hardness of Comp-B_4C-x%$MoSi_2$ as a function of the proportion of $MoSi_2$ aids (x=35–50 vol.%). The mean values and standard deviations reported are of ten separate measurements.

tains residual $MoSi_2$ [7] so that Comp-B_4C-x%$MoSi_2$ ($x \geq 35$) SPS-ed at 1400–1700 °C would still contain $MoSi_2$. Indeed, at this point, the optimal approach is hence to densify Comp-B_4C-20%$MoSi_2$, not Comp-B_4C-40%$MoSi_2$, at ~1700 °C to thus maximize the hardness [7]. And fourth, consuming all the $MoSi_2$ to form more β-SiC and β-MoB_2 is unreasonable because more B_4C will also be consumed and unreacted excess Si would likely form, which would complicate the SPS cycles without any hardness benefit. Therefore, residual $MoSi_2$ is a price to pay for the lower-temperature SPS of these B_4C composites. Nonetheless, $MoSi_2$ in the microstructures is not a major concern if Comp-B_4C-x%$MoSi_2$ (x=35–50) are very hard.

Fig. 3 shows the hardness of Comp-B_4C-x%$MoSi_2$ (x=35–50) determined by Vickers indentation (MV-1, Matsuzawa) at 98 N load. It is seen that the four have hardnesses of 20 GPa or greater, attributable to their phase composition dominated by covalent carbides (*i.e.*, B_4C and SiC) and transition-metal diborides (*i.e.*, MoB_2) as well as to their fine-grained microstructures. Therefore, this demonstrates the feasibility of fabricating very hard B_4C composites by ultra-low temperature SPS with $MoSi_2$ aids, in the sense that 1400 °C represents a homologous temperature for B_4C of only ~0.56 (because the B_4C melting point is ~2490 °C). It is also seen

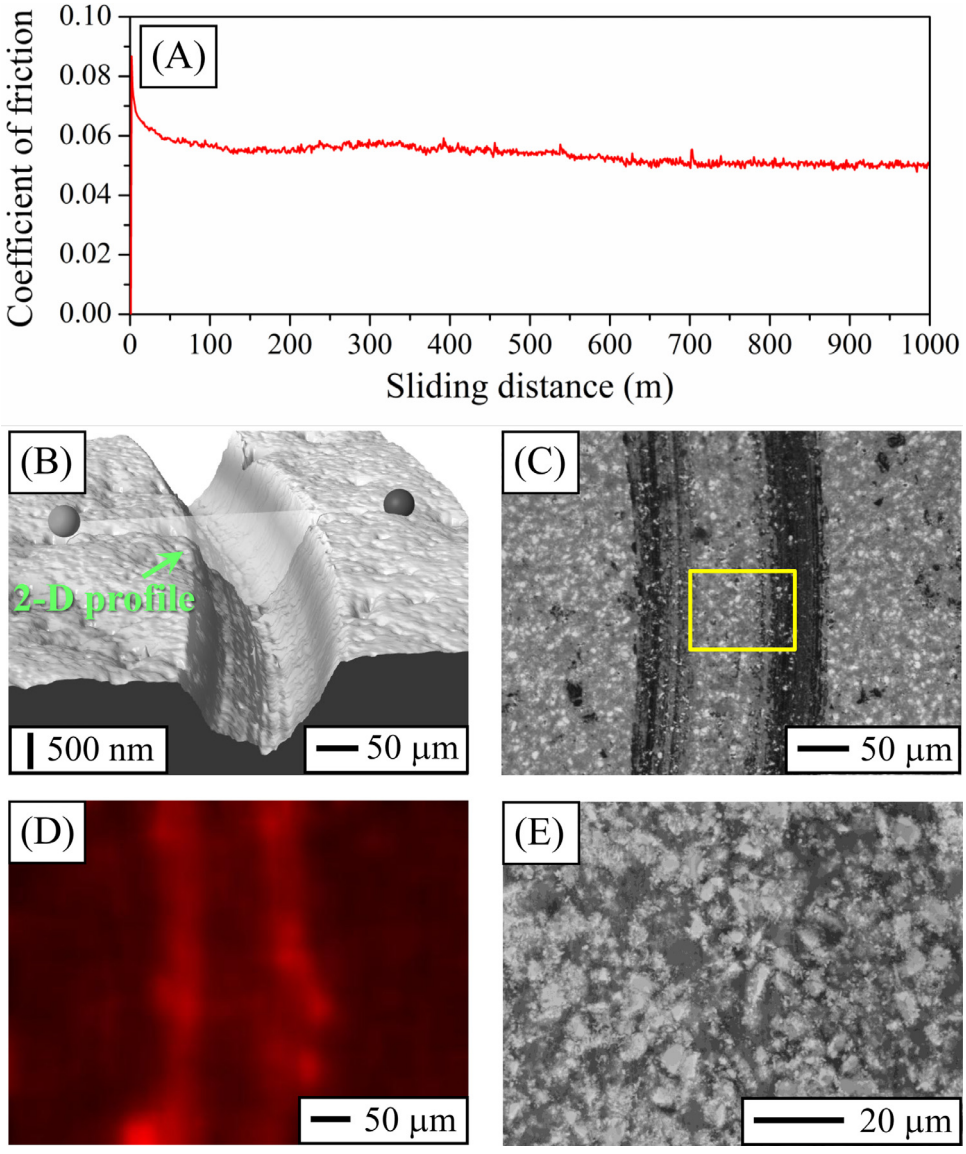

Fig. 4. Compendium of results deriving from the sliding-wear tests for Comp-B_4C-40%$MoSi_2$. (A) Friction curve measured as a function of the distance slid, (B) 3-D image and 2-D profile representative of the wear track, obtained by optical profilometry, (C) OM image showing the damage at the macro-scale, (D) elemental composition map of O inside and outside the wear track, obtained by EDS in the SEM, and (E) moderate-magnification SEM image showing the interior of the wear track at the micro-scale, at the location indicated in (C). Imaging (3-D profilometry, OM, and SEM/EDS at 30 kV with secondary electrons) was done at the conclusion of the wear tests.

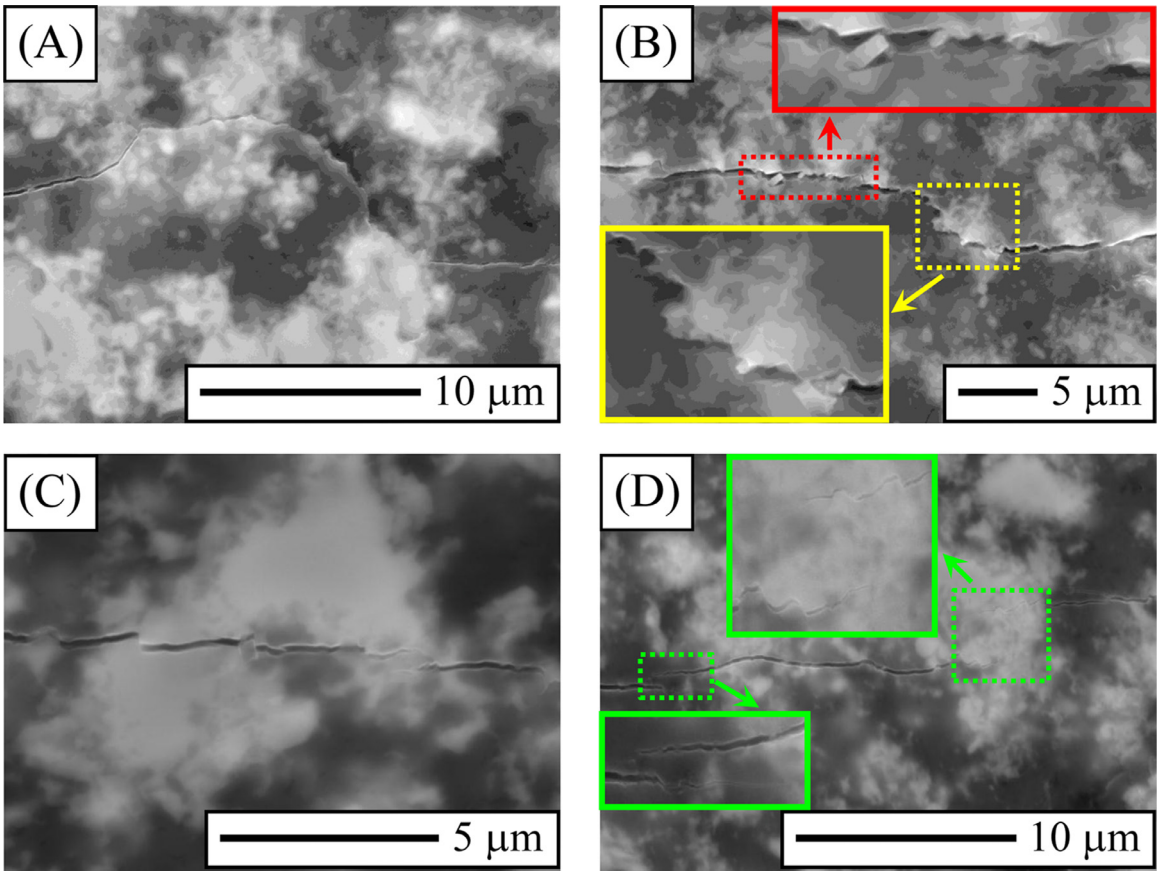

Fig. 5. SEM images representative of the crack propagation in the polished surface of Comp-B_4C-40%$MoSi_2$. (A) A crack being markedly deflected, (B) a crack being bridged and deflected, (C) a crack propagating inside a second-phase cluster while being bridged, and (D) a crack suffering evident branching (marked with arrows). The insets in (B) show specific details. Imaging was done with secondary electrons at 30 kV.

that the hardness of Comp-B_4C-x%$MoSi_2$ (x=35–50) first increases and then decreases with increasing proportion of $MoSi_2$ aids, being optimal for 40 vol.% $MoSi_2$ (*i.e.*, ~23 GPa). Thus, Comp-B_4C-35%$MoSi_2$ is, despite its greater content of ultrahard B_4C, somewhat softer than Comp-B_4C-40%$MoSi_2$ due to its slight porosity, and Comp-B_4C-45%$MoSi_2$ and Comp-B_4C-50%$MoSi_2$ are so as well due to their increasing contents of softer β-SiC, β-MoB_2, and $MoSi_2$. Importantly, Comp-B_4C-x%$MoSi_2$ (x=35–50), and particularly Comp-B_4C-40%$MoSi_2$, are much harder than the typical widely used oxide structural ceramics (*e.g.*, Y-TZP (<16 GPa) [17,18], $MgAl_2O_4$ (<17 GPa) [19,20], Al_2O_3 (<18 GPa) [21,22], *etc.*) fabricated at similar or slightly higher temperatures (*i.e.*, ~1300–1500 °C) and harder than, or at least as hard as, other non-oxide structural ceramics (*e.g.*, LPS-ed SiC (<24 GPa) [23,24], LPS-ed Si_3N_4 (<19 GPa) [25], *etc.*). fabricated at much higher temperatures (*i.e.*, >1800 °C).

Fig. 4 shows relevant results deriving from pin-on-disk wear tests (THT1000, Anton Paar) performed on Comp-B_4C-40%$MoSi_2$, the hardest of the present four Comp-B_4C-x%$MoSi_2$ (x=35–50), in ambient conditions at 40 N load, 12.5 mm/s linear sliding speed, 2-mm track radius, and 1000 m sliding distance, with 6.02 mm diameter diamond-coated SiC counter-balls (Dball G10, Nova Diamant). It is seen in Fig. 4A that the steady-state coefficient of friction is only ~0.053(3), indicating a smooth contact surface due to the absence of porosity in the material. According to the 3-D images obtained by optical profilometry (Profilm 3D, Filmetric), a typical one shown in Fig. 4B, even after sliding for 1000 m the wear scar remains very shallow (*i.e.*, depth of ~0.7 μm). The wear volume calculated from representative 2-D scar profiles (Fig. 4B) is only ~0.00197(1) mm^3, which results in a specific wear rate (SWR) as low as ~$4.92(3)\cdot10^{-8}$ $mm^3/(N\cdot m)$ (*i.e.*, a wear resistance as great as ~$2.03(1)\cdot10^7$ $(N\cdot m)/mm^3$), well within the realm of mild wear [26]. Importantly, Comp-B_4C-40%$MoSi_2$ thus wears essentially as slowly (SWR in the order of 10^{-8} $mm^3/(N\cdot m)$) as other ultrahard B_4C–based materials SPS-ed at much higher temperatures do [7,12].[5] Consistently with the low SWR, the surface of the wear track appears, as seen by optical microscopy (Epiphot 300, Nikon) in Fig. 4C, quite smooth (*i.e.*, polished) and shows only light abrasion, with microscopic wear markings consisting mostly of mild scratches by plastic deformation caused by the asperities of the counter-sphere [27,28]. Also, there is formation of a discontinuous oxide tribolayer (confirmed in Supplementary Fig. SI3), located near the edges where the contact stresses are higher [29], which contributed to the very low wear. The oxidic nature of the tribolayer indicates that no SiC, MoB_2, or $MoSi_2$ particles were pulled out from the material microstructure and smeared onto the wear track. Indeed, no evidence of grain pull-out is observed within the wear track in the higher-magnification SEM image of Fig. 4E (confirmed in Supplementary Fig. SI4). Thus, these novel B_4C composites wear according to the mode/mechanism already observed for other ultrahard B_4C–based materials (*i.e.*, by two-body abrasion dominated by plastic deformation).

The question may then arise as to why Comp-B_4C-40%$MoSi_2$ is in principle more appealing than a possible B_4C composite SPS-ed

[5] For example, also tested at 40 N for 1000 m, Comp-B_4C-20%$MoSi_2$ SPS-ed at 1700 °C, with ~33 GPa hardness, wore at ~$3.73\cdot10^{-8}$ $mm^3/(N\cdot m)$ [7]; a monolithic B_4C ceramic SPS-ed at 2100 °C, with ~32 GPa hardness, did so at ~$3.8\cdot10^{-8}$ $mm^3/(N\cdot m)$ [12]; and a B_4C composite SPS-ed at 1800 °C using 7 vol.% Ti-Al aids, with ~33 GPa hardness, did so at ~$3.1\cdot10^{-8}$ $mm^3/(N\cdot m)$ [12].

at 1400 °C using ~15–26 vol.% Si aids, as required to achieve full densification (not yet attempted).[6] Even though the B_4C-Si composite would likely be harder than Comp-B_4C-40%$MoSi_2$ due to its higher B_4C content (~85–74 *vs* ~40 vol.%), the fact is that Comp-B_4C-40%$MoSi_2$ is sufficiently hard and presumably much tougher, and this latter is also a highly desirable attribute given the brittleness of B_4C materials [2,3,30]. Indeed, as observed for other B_4C composites with carbide and/or boride second phases [5–8,33–38], the singular multi-particulate microstructure of Comp-B_4C-40%$MoSi_2$ (and of Comp-B_4C-*x*%$MoSi_2$ (*x*=35–50)) must offer major impedance to crack advance because the SiC and MoB_2 grains/clusters formed *in situ* during SPS, as well as the residual $MoSi_2$ grains, will act as toughening phases. In this regard, Fig. 5 shows SEM images representative of how tortuously the radial cracks emanating from the Vickers indent corners propagate through Comp-B_4C-40%$MoSi_2$ due to the occurrence of crack deflection (Fig. 5A,B), bridging (Fig. 5B,C), and branching (Fig. 5D), with an estimated fracture toughness of 4.5–5 MPa·$m^{1/2}$ which is twice that of the B_4C monoliths [30]. Therefore, besides being very hard and super wear-resistant, Comp-B_4C-40%$MoSi_2$ is also toughened, which is a long-sought-for synergy in B_4C materials for structural applications.

With these results in mind, future work should thus be directed towards the challenge of fabricating these novel B_4C composites, ideally nanostructured or with ultrafine-grained microstructures, by near-net-shape manufacture [9,11,39–42] and (conventional and ultrafast) low-temperature pressureless sintering. This would pave the way towards facilitating their industrial scalability, even with them having improved mechanical/tribological properties if the grain size is more refined. However, achieving this will require the development of B_4C+$MoSi_2$ suspensions or pastes suitable for the wet shaping of green parts and the optimization of their sintering cycles, tasks which, however, lie beyond the scope of the present study.

Declaration of Competing Interest

The authors declare that they have no known competing financial interests or personal relationships that could have appeared to influence the work reported in this paper.

Acknowledgments

This work was supported by the Junta de Extremadura under Grants nos. IB20017, TA18014, and GR18149 (co-financed with FEDER Funds).

Supplementary materials

Supplementary material associated with this article can be found, in the online version, at doi:10.1016/j.scriptamat.2022.114516.

References

[1] R. Riedel, Handbook of Ceramic Hard Materials, Wiley-VCH, Weinheim, 2000.
[2] V. Kanyanta, Microstructure-Property Correlations for Hard, Superhard, and Ultrahard Materials, Springer International Publishing, 2016.
[3] F. Thevenot, J. Eur. Ceram. Soc. 6 (4) (1990) 205–225.
[4] A.K. Suri, C. Subramanian, J.K. Sonber, T.S.R.Ch. Murthy, Int. Mater. Rev. 55 (1) (2010) 4–40.
[5] C. Ojalvo, F. Guiberteau, A.L. Ortiz, J. Eur. Ceram. Soc. 39 (9) (2019) 2862–2873.
[6] Y. Wang, Q. Liu, B. Zhang, H. Zhang, Y. Jin, Z. Zhong, J. Ye, Y. Ren, F. Ye, W. Wang, Ceram. Int. 47 (8) (2021) 10665–10671.
[7] V. Zamora, C. Ojalvo, F. Guiberteau, O. Borrero-López, A.L. Ortiz, J. Eur. Ceram. Soc. 41 (16) (2021) 68–75.
[8] W. Ji, R.I. Todd, W. Wang, H. Wang, J. Zhang, Z. Fu, J. Eur. Ceram. Soc. 36 (10) (2016) 2419–2426.
[9] C. Ojalvo, R. Moreno, F. Guiberteau, A.L. Ortiz, J. Eur. Ceram. Soc. 40 (2) (2020) 226–233.
[10] C. Ojalvo, R. Moreno, F. Guiberteau, A.L. Ortiz, J. Eur. Ceram. Soc. 40 (9) (2020) 3406–3413.
[11] C. Ojalvo, R. Moreno, F. Guiberteau, A.L. Ortiz, J. Eur. Ceram. Soc. 40 (12) (2020) 4354–4360.
[12] C. Ojalvo, E. Sánchez-González, F. Guiberteau, O. Borrero-López, A.L. Ortiz, J. Eur. Ceram. Soc. 40 (15) (2020) 5286–5292.
[13] A.L. Ortiz, C.A. Galán, O. Borrero-López, F. Guiberteau, Scr. Mater. 177 (2020) 91–95.
[14] C. Ojalvo, V. Zamora, R. Moreno, F. Guiberteau, A.L. Ortiz, J. Eur. Ceram. Soc. 41 (3) (2021) 1869–1877.
[15] R.M. German, Sintering Theory and Practice, Wiley, New York, 1996.
[16] R.M. German, Liquid Phase Sintering, Plenum Press, New York, US, 1985.
[17] J. Alonso, F. Rodríguez-Rojas, O. Borrero-López, A.L. Ortiz, F. Guiberteau, Int. J. Appl. Ceram. Technol. 16 (5) (2019) 1954–1961 17.
[18] F. Rodríguez-Rojas, R. Cano-Crespo, O. Borrero-López, A. Domínguez-Rodríguez, A.L. Ortiz, J. Eur. Ceram. Soc. 41 (6) (2021) 3595–3602.
[19] T. Mroz, L.M. Goldman, A.D. Gledhill, D. Li, N.P. Padture, Int. J. Appl. Ceram. Technol. 9 (1) (2012) 83–90.
[20] O. Borrero-López, A.L. Ortiz, A.D. Gledhill, F. Guiberteau, T. Mroz, L.M. Goldman, N.P. Padture, J. Eur. Ceram. Soc. 32 (12) (2012) 3143–3149.
[21] R.G. Munro, J. Am. Ceram. Soc. 80 (8) (1997) 1919–1928.
[22] Q. Wang, C. Ramírez, C.S. Watts, O. Borrero-López, A.L. Ortiz, B.W. Sheldon, N.P. Padture, Acta Mater. 186 (2020) 29–39.
[23] O. Borrero-López, A.L. Ortiz, F. Guiberteau, N.P. Padture, J. Eur. Ceram. Soc. 27 (11) (2007) 3351–3357.
[24] M. Khodaei, O. Yaghobizadeh, S.H.N. Alhosseini, S. Esmaeeli, S.R. Mousavi, J. Eur. Ceram. Soc. 39 (7) (2019) 2215–2231.
[25] M. Kašiarová, P. Tatarko, P. Burik, J. Dusza, P. Šajgalík, J. Eur. Ceram. Soc. 34 (14) (2014) 3301–3308.
[26] G. Stachowiak, A.W. Batchelor, Engineering Tribology, 3rd Edition, Elsevier Butterworth-Heinemann, Oxford, UK, 2005.
[27] O. Borrero-López, A. Pajares, P. Constantino, B.R. Lawn, Acta Biomater. 14 (2015) 146–153.
[28] B.R. Lawn, O. Borrero-Lopez, H. Huang, Y. Zhang, J. Am. Ceram. Soc. 104 (1) (2021) 5–22.
[29] G.M. Hamilton, L.E. Goodman, J. Appl. Mech. 33 (2) (1966) 371–376.
[30] B.M. Moshtaghioun, D. Gómez-García, A. Domínguez-Rodríguez, R.I. Todd, J. Eur. Ceram. Soc. 36 (7) (2016) 1829–1834.
[31] S.S. Rehman, W. Ji, S.A. Khan, Z. Fun, F. Zhang, Ceram. Int. 41 (1 Part B) (2015) 1903–1906.
[32] L. Ma, K.Y. Xie, M.F. Toksoy, K. Kuwelkar, R.A. Haber, K.J. Hemker, Mater. Charact. 134 (2017) 274–278.
[33] W.G. Fahrenholtz, E.W. Neuman, H.J. Brown-Shaklee, G.E. Hilmas, J. Am. Ceram. Soc. 93 (11) (2010) 3580–3583.
[34] B.M. Moshtaghioun, A.L. Ortiz, D. Gómez-García, A. Domínguez-Rodríguez, J. Eur. Ceram. Soc. 33 (8) (2013) 1395–1401 34.
[35] X. Zhang, Z. Zhang, W. Wang, J. Shan, H. Che, J. Mu, G. Wang, J. Am. Ceram. Soc. 100 (7) (2017) 3099–3107.
[36] Q. Wen, Y. Tan, Z. Zhong, H. Zhang, X. Zhou, Mater. Sci. Eng. A 701 (2017) 338–343.
[37] E.W. Neuman, H.J. Brown-Shaklee, G.E. Hilmas, W.G. Fahrenholtz, J. Am. Ceram. Soc. 101 (2) (2018) 497–501.
[38] X. Zhang, Z. Zhang, W. Wang, X. Zhang, J. Mu, G. Wang, Z. Fu, J. Eur. Ceram. Soc. 37 (2) (2017) 865–869.
[39] F. Rodríguez-Rojas, R. Moreno, F. Guiberteau, A.L. Ortiz, J. Eur. Ceram. Soc. 36 (8) (2016) 1915–1921.
[40] A.L. Ortiz, V.M. Candelario, R. Moreno, F. Guiberteau, J. Eur. Ceram. Soc. 37 (15) (2017) 4577–4584.
[41] C. Ojalvo, M. Ayllón, A.L. Ortiz, R. Moreno, J. Eur. Ceram. Soc. 41 (11) (2021) 5457–5465 41.
[42] S. Eqtesadi, A. Motealleh, F.H. Perera, P. Miranda, A. Pajares, R. Wendelbo, F. Guiberteau, Scr. Mater. 145 (2018) 14–18.

[6] B_4C-Si composites have already been SPS-ed, but using much lower proportions of Si aids (*i.e.*, 4–10 wt.%, equivalent to ~4.3–10.7 vol.%) and much higher temperatures (*i.e.*, 1700 °C) [31,32]. They have a fracture toughness of ~2.4 MPa·$m^{1/2}$ [32].